Molecular Biology of the Cell
Vol. 16, 4852–4866, October 2005

Helicobacter pylori VacA Cytotoxin: A Probe for a Clathrin-independent and Cdc42-dependent Pinocytic Pathway Routed to Late Endosomes[D] [V]

Nils C. Gauthier,* Pascale Monzo,† Vincent Kaddai,† Anne Doye,* Vittorio Ricci,‡ and Patrice Boquet*

*INSERM U 627 and †INSERM U 568, IFR 50, Faculté de Médecine, 06107 Nice, France; and ‡Human Physiology Section, Department of Experimental Medicine, University of Pavia, 27100 Pavia, Italy

Submitted May 5, 2005; Revised June 24, 2005; Accepted July 19, 2005
Monitoring Editor: Howard Riezman

The vacuolating cytotoxin VacA is a major virulence factor of *Helicobacter pylori*, a bacterium responsible for gastroduodenal ulcers and cancer. VacA associates with lipid rafts, is endocytosed, and reaches the late endocytic compartment where it induces vacuolation. We have investigated the endocytic and intracellular trafficking pathways used by VacA, in HeLa and gastric AGS cells. We report here that VacA was first bound to plasma-membrane domains localized above F-actin structures that were controlled by the Rac1 GTPase. VacA was subsequently pinocytosed by a clathrin-independent mechanism into cell peripheral early endocytic compartments lacking caveolin 1, the Rab5 effector early endosomes antigen-1 (EEA1) and transferrin. These compartments took up fluid-phase (as evidenced by the accumulation of fluorescent dextran) and glycosylphosphatidylinositol-anchored proteins (GPI-APs). VacA pinocytosis was controlled by Cdc42 and did not require cellular tyrosine kinases, dynamin 2, ADP-ribosylating factor 6, or RhoA GTPase activities. VacA was subsequently routed to EEA1-sorting endosomes and then sorted to late endosomes. During all these different endocytic steps, VacA was continuously associated with detergent resistant membrane domains. From these results we propose that VacA might be a valuable probe to study raft-associated molecules, pinocytosed by a clathrin-independent mechanism, and routed to the degradative compartment.

INTRODUCTION

Gastric infection by *Helicobacter pylori* is associated with chronic gastritis, peptic ulceration, and gastric cancer in humans (Blaser and Atherton, 2004). Among different virulence factors of *H. pylori*, such as those encoded by the cag pathogenicity island, the BabA adhesin or urease, the VacA cytotoxin (Leunk *et al.*, 1988; Cover, 1996; Boquet *et al.*, 2003; Cover and Blanke, 2005) is an important pathogenic determinant involved in the bacterial colonization of the stomach (Salama *et al.*, 2001).

The mature VacA cytotoxin (M_r: 90 kDa) exhibits the structure of an A-B toxin with a N-terminal (p34; M_r: 34 kDa) and a C-terminal (p58; M_r: 58 kDa) subunit, with an exposed protease-sensitive loop between these two fragments (Cover, 1996). The p34 fragment contains a short N-terminus hydrophobic domain required for vacuolation and thus may be assimilated to the effector domain (A) of an A-B toxin (Boquet *et al.*, 2003; Cover and Blanke, 2005). The p58 subunit (B) is responsible for the cytotoxin binding to the cell (Garner and Cover, 1996) through a motif localized in the middle of p58 (Pagliaccia *et al.*, 1998). VacA binds on one or several receptor (s) to the cell plasma membrane (Cover and Blanke, 2005). Monomers of VacA oligomerize in the plane of artificial lipid bilayers, or in the cell plasma membrane, to form anionic channels (Czajkowsky *et al.*, 1999; Szabo *et al.*, 1999; Tombola *et al.*, 1999; Gauthier *et al.*, 2004). VacA channels are subsequently endocytosed (Gauthier *et al.*, 2004) and reach their final endocytic destination, the late endosomes (Papini *et al.*, 1994; Ricci *et al.*, 1997). The VacA channel, by inducing a chloride ions influx into late endosomes, activates the proton pump vATPase, leading to the accumulation of osmotic species such as NH_4Cl, and results in late endosomes swelling (Papini *et al.*, 2001; Gauthier *et al.*, 2004; Cover and Blanke, 2005). The cytotoxin also could escapes from endosomes to the cytosol to target mitochondria (Galmiche *et al.*, 2000; Willhite and Blanke, 2004; Blanke, 2005; Cover and Blanke, 2005).

Interestingly, the exact intracellular pathway followed by the cytoxin has not yet been deciphered. Using VacA-induced vacuolation as an experimental readout of the cytotoxin internalization as well as the inhibitors of clathrin function such as the dominant-negative mutant forms of Eps 15, dynamin 2, and intersectin, we have previously shown that, in epithelial HEp2 cells, VacA activity is not blocked when the clathrin- or dynamin-dependent pathways of endocytosis are inhibited (Ricci *et al.*, 2000). Furthermore, VacA-induced vacuolation is highly sensitive to the disruption of the actin cytoskeleton (Ricci *et al.*, 2000; Gauthier *et al.*, 2004; Li *et al.*, 2004). These data support the notion that VacA may be endocytosed through an actin-dependent pathway that is independent of both clathrin and dynamin (Ricci *et al.*, 2000).

This article was published online ahead of print in *MBC in Press* (http://www.molbiolcell.org/cgi/doi/10.1091/mbc.E05–05–0398) on July 29, 2005.

[D] [V] The online version of this article contains supplemental material at *MBC Online* (http://www.molbiolcell.org).

Address correspondence to: Patrice Boquet (boquet@unice.fr).

VacA associates with lipid rafts (Patel *et al.*, 2002; Schraw *et al.*, 2002; Gauthier *et al.*, 2004) and requires cholesterol for cell binding and internalization (Patel *et al.*, 2002; Schraw *et al.*, 2002) as well as glycosylphosphatidylinositol-anchored proteins (GPI-APs) for its full vacuolating activity (Ricci *et al.*, 2000; Kuo and Wang, 2003; Gauthier *et al.*, 2004). However, in all likelihood GPI-APs, which are components of lipid rafts, are not the cell surface receptors for VacA (Schraw *et al.*, 2002; Kuo and Wang, 2003; Gauthier *et al.*, 2004). Lipid rafts represent highly ordered, rigid lipid microdomains thought to be mostly, but not solely, internalized by clathrin-independent pathways. An increasing number of different endocytic pathways have been described for lipid rafts (Conner and Schmid, 2003; Parton and Richards, 2003; Mayor and Riezman, 2004). Importantly, different cell invasive pathogenic bacteria or their virulence factors have been shown to use lipid rafts to interact with host cells (Lafont *et al.*, 2004). VacA may thus constitute an invaluable marker for dissecting one of these, not yet well characterized endocytic mechanisms for lipid rafts.

In the present study, using purified VacA, we have investigated the mechanism by which this lipid raft-associated cytotoxin binds to the cell surface, is endocytosed, and subsequently, routed to the degradative compartments, in HeLa and gastric epithelial AGS cells.

MATERIALS AND METHODS

Cell Lines, Bacterial Strain, Plasmids, Toxins, and Antibodies

HeLa (from a human cervix carcinoma, a gift of T. L. Cover, Vanderbilt University, TN) and AGS (from a human gastric carcinoma, ATCC number: CRLt-1739) cells were cultured and transfected as previously described (Ricci *et al.*, 2000). Eukaryotic plasmid vectors used in this work are as follows: HA Rac Q61L and HA Rac T17N (Doye *et al.*, 2002), myc-Cdc42 T17N (J. de Gunsburg, Institut Curie, Paris, France), GFP-ADP-ribosylating factor 6 (Arf6 WT) and GFP-ADP-ribosylating factor 6 mutant (Arf6 N122I; M. Franco, CNRS, Sophia Antipolis, France), GFP-Dyn2 K44A (S. Schmid, Scripps Research Institute, La Jolla, CA), and GFP-Eps15 mutant (ED95/295, A. Benmerah, INSERM U567, Paris, France). Both the decay-accelerating factor (DAF) DNA fused to the GFP (used as a GPI-AP and termed throughout this work GPI-GFP), and the DNA of caveolin 1 fused to the GFP (used as a GFP-caveolin 1) were from A. Galmiche (Max Plank Inst. für Infektionsbiologie, Berlin, Germany). VacA was purified from the *H. pylori* 60190 strain (ATCC 49503), according to Cover and Blaser (1992). Immediately before use on cells, purified VacA (2 μg/ml in all this work) was acid-activated as described (de Bernard *et al.*, 1995). The *Clostridium botulinum* C3 transferase (Boquet and Lemichez, 2003) was produced as a recombinant protein. The nontoxic double mutant aerolysin pan-GPI-APs marker ASSP-Alexa-546 (ASSP-546; Fivaz *et al.*, 2002) was a gift of F. G. van der Goot (University of Geneva, Switzerland). The cholera toxin B subunit (CTxB) and the monoclonal antibody (Mab) directed against the CTxB subunit (Mab LT39) were both from C. Czerkinsky and F. Anjuere (INSERM U 721, Nice, France). The rabbit polyclonal IgG 958 anti-VacA was a gift of T. L. Cover. This antibody, directed against the carboxy-terminal domain of the VacA p58 fragment (Garner and Cover, 1996), was used throughout this work. This antibody did not react with HeLa cells by immunofluorescence as previously shown by Garner and Cover (1996) as well as with AGS cells (Supplementary Figure 1, A and B). The Mab anti-human transferrin receptor (Mab 68.4) was from Zymed (South San Francisco, CA). The Mab anti-early endosomes antigen-1 (EEA1; clone 14) and Mab anti-flotillin-1 were from BD Biosciences (Le Pont de Claix, France). The Mab anti-caveolin 1 (clone C060) (Transduction Laboratories, Lexington, KY) reacted against a major M_w 22-kDa band (caveolin 1) by Western blot in both HeLa and AGS cells (unpublished data). The Mab anti-HA (clone 16B12) and the Mab anti-myc (clone 9E10) were from Babco (Richmond, CA). Texas red-labeled and Cy5-labeled secondary antibodies against rabbit IgG were purchased from Molecular Probes (Eugene, OR) and anti-mouse secondary antibodies labeled with FITC or Cy5 from Dako (A/S, Denmark). Phalloidin-FITC and -TRITC were from Sigma-Aldrich (Saint-Quentin Fallavier, France). Texas red-labeled or FITC-labeled 70 kDa-dextran (Txrd-dextran, FITC-dextran), FITC-wheat germ agglutinin (FITC-WGA), Texas red-labeled transferrin (Txrd-TF), FITC-transferrin (FITC-TF) were from Molecular Probes. Epidermal growth factor (EGF) was from Sigma-Aldrich and the anti-phosphotyrosine Mab (P-Tyr-100 sample 9411) from Cell Signaling (Beverly, MA). Methyl-β-cyclodextrin and filipin were from Sigma-Aldrich.

Treatment of Cells with Cytochalasin D, Genistein, Exoenzyme C3, Amiloride, and Phorbol 12-myristate 13-acetate

The treatment of cells with cytochalasin D (Sigma-Aldrich) has been described previously (Ricci *et al.*, 2000; Gauthier *et al.*, 2004). The tyrosine kinase inhibitor genistein (Sigma-Aldrich) was used at 100 μg/ml and the activity of the drug was controlled by its ability to block tyrosine phosphorylations located in focal adhesion points (unpublished data). Amiloride (Sigma-Aldrich) was used at 10 μg/ml, and the activity of the drug was controlled by its ability to decrease phorbol 12-myristate 13-acetate (TPA)-induced macropinocytosis (unpublished data). Cells were pretreated for 30 min at 37°C with genistein before their transfer to 4°C. VacA was added in cold medium for 1 h, rinsed, and transferred to warm medium in the presence of genistein or amiloride for 30 min, fixed, and analyzed for VacA immunofluorescence. The TPA (Sigma-Aldrich) was added to cells in DMEM at a final concentration of 30 nM for 30 min at 37°C to induce macropinocytosis. The C3 exoenzyme was added to cells at 50 μg/ml for 18 h. The activity of C3 on RhoA was controlled by its ability to block stress fiber formation (unpublished data). Cells were then processed as described for the genistein and amiloride treatments.

Analysis of Lipid Rafts by Density Gradient

AGS cells (3×10^6) were plated in 100-mm diameter tissue culture dishes 24 h before use. Activated-VacA was added to cells at 2 μg/ml for 1 h in DMEM-HEPES at 4°C. Cells were washed and transferred into warmed DMEM (37°C) for the indicated periods of time. After triple rinsing with ice-cold phosphate-buffered saline (PBS), cells were scraped off the dishes in calcium-free PBS and centrifuged (1000 $\times$ *g*, 5 min, 4°C). Cells were lysed 30 min at 4°C in TNE buffer (25 mM Tris-HCl, pH 7.4, 150 mM NaCl, 5 mM EDTA) containing 1% Triton X-100 and a mix of protease inhibitors (Complete EDTA-free, Roche, Basel, Switzerland). Optiprep 60 (Axis-Shield, Oslo, Norway) was added to the lysate supernatant at the bottom of an ultracentrifuge tube (Beckman, Palo Alto, CA) to obtain a 40% final concentration. A layer of Optiprep 30% (Optiprep 60 diluted in TNE) and a final layer of TNE were added. On centrifugation (100,000 $\times$ *g*, 2 h, 4°C), 10 fractions from the top to the bottom of the tube were collected. Identical volumes of each fraction were analyzed by SDS-PAGE and immunoblotting.

Association of VacA in Endocytic Compartments with Detergent-insoluble Membranes

After VacA binding and upon pinocytosis of the cytotoxin for the different periods of time, AGS cells grown on coverslips where rinsed at 4°C in PBS containing calcium and magnesium and immersed for 30 s at 4°C in 4 separate baths of 50 mM MES, 3 mM EGTA, 5 mM $MgCl_2$ (pH 6.4) containing or not 0.5% Triton X-100. After these treatments, cells were immediately fixed and processed for immunofluorescence studies. For quantification by immunoblotting, AGS cells, grown on plastic dishes, were submitted to the same treatments but lysed instead of being fixed. Identical volume of lysates were analyzed by SDS-PAGE and immunoblotting.

Immunofluorescence Studies

Immunofluorescence studies were performed as previously described (Ricci *et al.*, 2000; Gauthier *et al.*, 2004). For LAMP1 and CTxB labeling, saponin (0.1%; Sigma-Aldrich) was used instead of Triton X-100 for permeabilization and all the immunofluorescence steps were performed using PBS containing 0.1% bovine serum albumin (Sigma-Aldrich) and 0.1% saponin. For 2D deconvolution or 3D reconstructions, fluorescence signals were analyzed using an Axiovert 200 microscope (Carl Zeiss, Göttingen, Germany) equipped with a shutter-controlled illumination system (Carl Zeiss) and a cooled digital CCD camera (Roper Scientific, Evry, France). Images were recorded and reconstructed using the Metamorph 2.0 image analysis software (Universal Imaging Corporation, Evry, France) and QuickTime pro5 (Apple, http://store-apple.com). For 3D reconstructions using confocal sections, the Image J software was used (http://rsb.info.nih.gov/ij/). For endocytic kinetics studies, VacA was incubated with cells for 1 h at 4°C in DMEM-HEPES. After three washes in cold DMEM, cells were transferred to either DMEM, cytochalasin D-DMEM, genistein-DMEM, C3-DMEM, or dextran-DMEM, prewarmed to 37°C, and incubated at the same temperature for the time indicated in each experiment. Cells were then analyzed by immunofluorescence. Transferrin endocytosis was monitored by FITC-TF or Txrd-TF: cells were serum-depleted (to promote the recycling of free transferrin receptors) by incubation in DMEM (15 min) and FITC-TF or Txrd-TF (200 μg/ml) was added at 4°C together with VacA for 1 h. The ASSP-546 (0.5 μg/ml) endocytosis was performed as described for transferrin but using non-serum-depleted cells.

Colocalization Index Method

Cells were analyzed by fluorescence and confocal microscopy and fully reconstructed to observe the total vesicles population. All positive vesicles for each endocytic markers used in this work were counted for each cell. Two

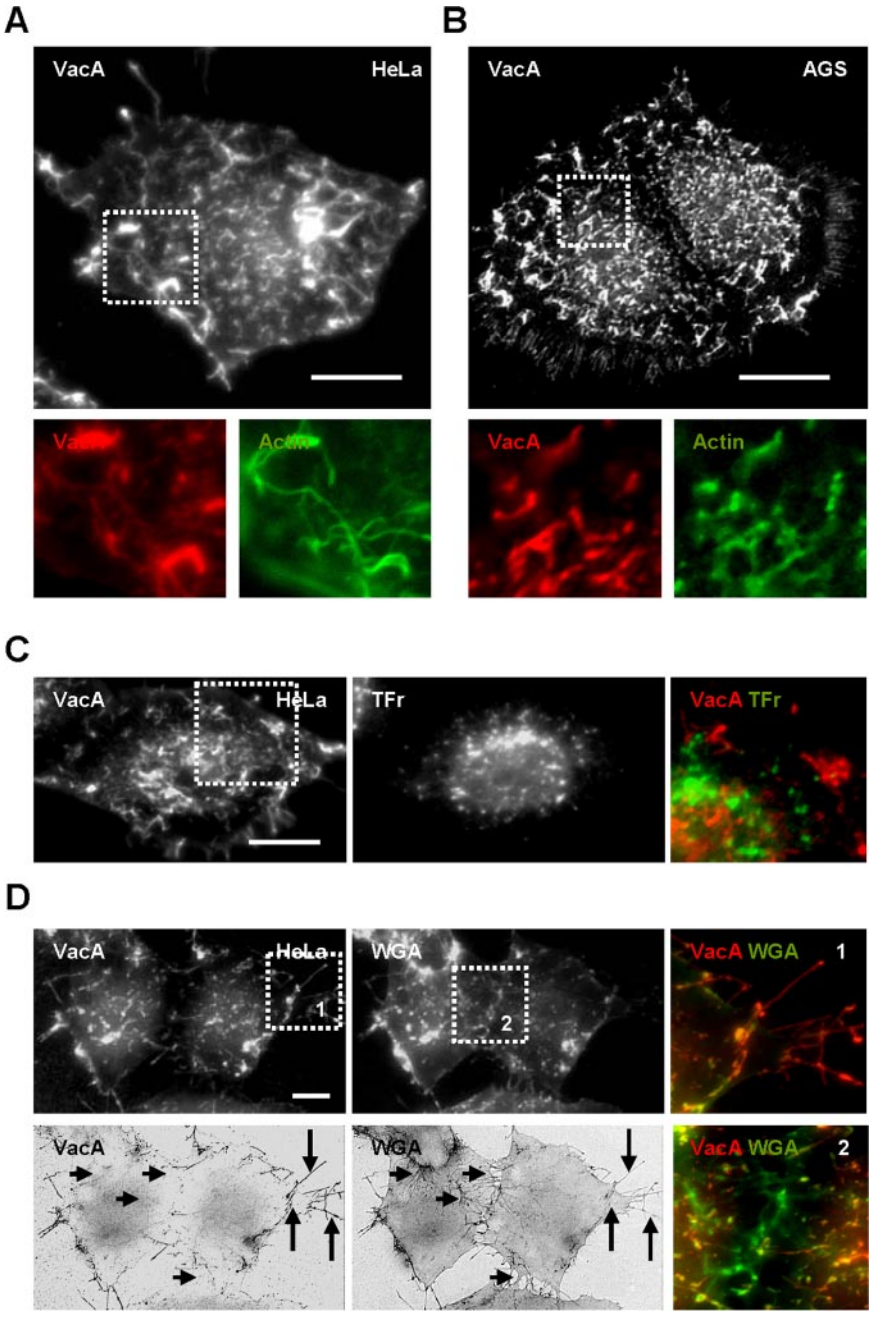

Figure 1. VacA binds membrane domains localized above F-actin structures on the surface of epithelial cells. HeLa cells (A, C, and D) or AGS cells (B) were incubated with VacA at 4°C for 1 h, washed, fixed, and processed for the detection of VacA by 3D-reconstructed indirect immunofluorescence using a video microscope. (A and B) Localization of VacA on membrane domains sustained by F-actin (FITC-phalloidin). VacA is shown alone in black and white in the full size cell pictures and in red in the zooms. Actin is shown in green in the zooms. For A and B see also Supplementary Videos 1 and 2. In C, surface membrane domains containing VacA or transferrin receptor (TFr; zoom, VacA: red, and TFR: green). In D, during the last 15 min of VacA binding at 4°C, cells were incubated with FITC-WGA before fixation in order to detect all cell surface details. The two upper pictures and zooms 1 and 2 represent 3D-reconstructed indirect VacA immunofluorescence or direct FITC-WGA fluorescence of cells. The two lower pictures represent the 2D-deconvoluted VacA and WGA fluorescence (in negative and black and white) of the cells basal plane. VacA is concentrated on certain membrane extensions (long arrows and zoom 1) unlike WGA that binds to the entire cell surface and is also found on retraction fibers observed in cell junctions (short arrows and zoom 2). Scale bars, 10 μm.

different markers that labeled the same vesicle were considered as colocalized. Results are expressed as colocalization indexes for which 1 represents 100% of colocalization between two endocytic markers. For example, the ASSP/VacA colocalization index represents the ratio of the number of ASSP-546 positive vesicles colocalized with VacA to the total number of vesicles containing ASSP-546 (with or without VacA). Conversely, the VacA/ASSP colocalization index is the ratio of the number of VacA-positive vesicles colocalized with ASSP-546 to the total number of vesicles containing VacA (with or without ASSP-546). Colocalization indexes were determined for each cell and the results represent the average value of n cells colocalization indexes (n is given in each figure).

RESULTS

VacA Binds Membrane Domains Localized above F-actin Structures

We first examined the plasma membrane structures on which VacA was associated at 4°C. When VacA was bound to HeLa (Figure 1A and Supplementary Video 1) or AGS (Figure 1B and Supplementary Video 2) cells for 1 h at 4°C, the cytotoxin was not uniformly associated with the cell surface but was mostly found on domains localized above F-actin structures, particularly on membrane extensions. No colocalization between the cytotoxin and either transferrin receptors (Figure 1C) or caveolin 1 (Supplementary Figure 1A) was observed at the level of the cell surface. Noteworthy, VacA was not associated with all cell membrane extensions decorated by a fluorescent lectin, a wheat germ agglutinin known to bind *N*-acetyl neuraminic acid and *N*-acetyl galactosamine residues (Adair and Kornfeld, 1974), but selectively associated with some of these structures located mostly at the cell leading edges (Figure 1D). Of note, the cytotoxin VacA was not bound on retraction fibers observed between cells (Figure 1D).

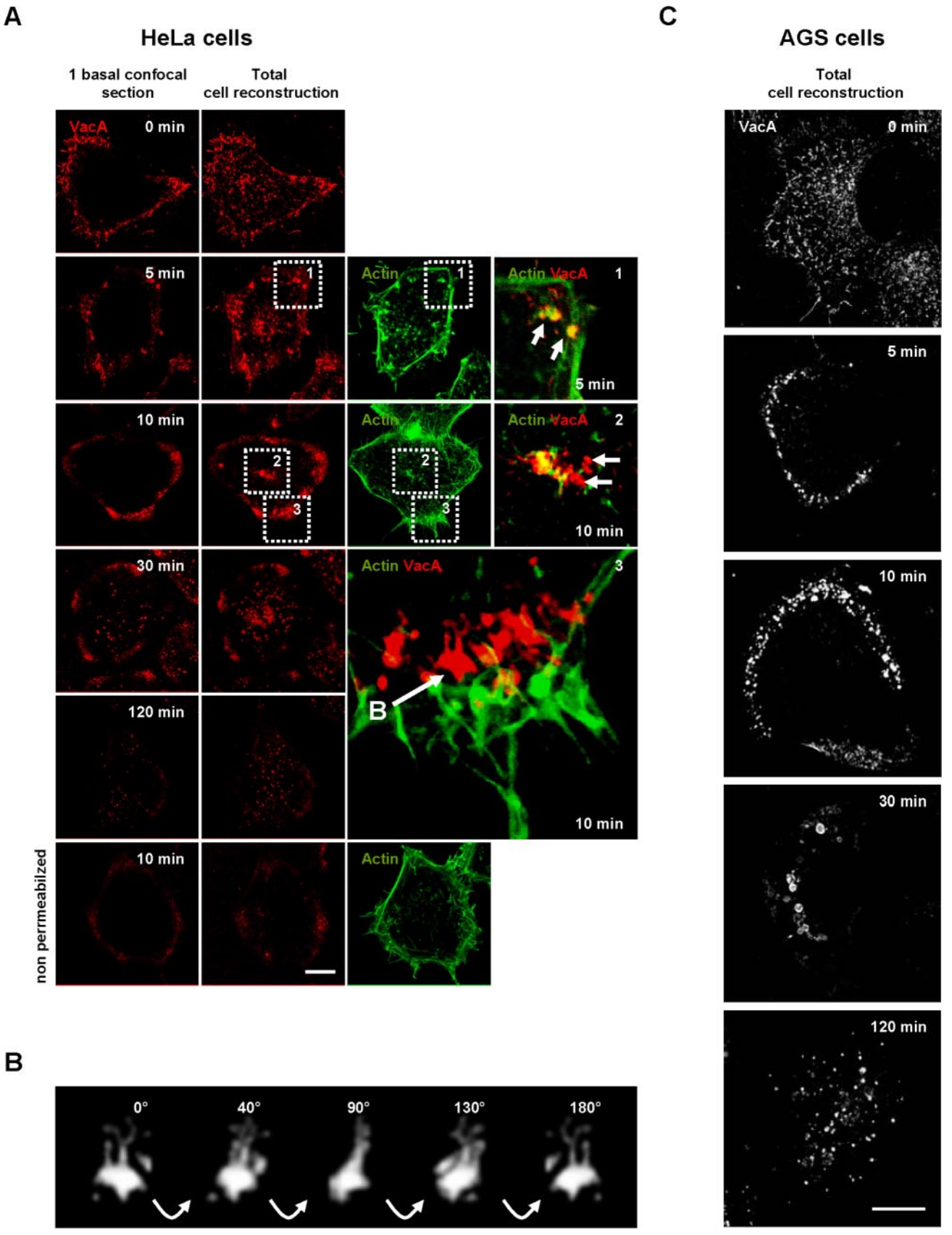

Figure 2. Time course of VacA endocytosis in HeLa cells. (A) HeLa cells were incubated with VacA at 4°C for 1 h, washed, and incubated for various periods of time at 37°C. Cells (permeabilized or not) were fixed, processed for the detection of VacA immunofluorescence, and observed by confocal microscopy. After 5 min, VacA (red) was concentrated in punctuate fluorescence patterns associated with F-actin (green;

Dynamic of VacA Internalization Process

We next examined the dynamics of the VacA internalization process. On transfer of HeLa cells to warm (37°C) medium, the toxin was taken up relatively rapidly. After 5 min at 37°C, cytotoxin molecules were already detected in intracellular vesicles (Figure 2 A). Of note, the transfer of the cells from 4 to 37°C likely overestimated the real timings of VacA internalization because of the rewarming process, as already suggested by Maxfield and McGraw (2004). VacA and F-actin were clearly found at the same location during the early steps of the entry process (Figure 2A, 5 min, zoom 1). Internalized cytotoxin molecules were surrounded with F-actin structures that appeared to entrap endocytosed VacA (Figure 2A, 5 min, zoom 1).

After 10 min of endocytosis, VacA was internalized into tubulovesicular intracellular compartments localized at the top of the cell (Figure 2A, 10 min, zoom 2) and predominantly at the cell basal periphery (Figure 2A, 10 min, zoom 3, and Supplementary Video 3; Figure 2B and Supplementary Video 4). Clearly, these structures were intracellular and not localized at the level of the cell surface because they were not detected in nonpermeabilized preparations (Figure 2A, 10 min, nonpermeabilized condition). VacA endocytosed for 10 min was not any longer closely associated with actin filaments (Figure 2A, zoom 3, and Supplementary Video 3). After 30 min at 37°C, some VacA-containing vesicles were observed scattered in the cytosol albeit the cell peripheral VacA-positive intracellular compartment still contained cytotoxin molecules (Figure 2A, 30 min). After 120 min at 37°C, VacA was only observed in vesicular structures scattered throughout the cytosol (Figure 2A, 120 min).

In AGS cells, VacA internalization appeared similar to that of HeLa cells. On 5 min of transfer to warm medium, most VacA molecules were localized to vesicular structures at the basal cell periphery (Figure 2C, 5 min). After 10 min of endocytosis VacA immunofluorescent signals increased in the basal cell peripheral compartments (Figure 2C, 10 min). Compared with HeLa cells, the AGS cell peripheral VacA-positive compartments were more polarized and no major accumulation of the cytotoxin could be observed in compartments at the top of the cell (Figure 2C and Supplementary Video 5). On 30 min of transfer of cells to 37°C, some large vesicles containing VacA, located slightly at the rear of the previous basal peripheral compartments in which VacA accumulated at early time points, were observed (Figure 2C, 30 min). At the same time, the basal cell peripheral VacA-positive compartments clearly disappeared (Figure 2C, 30 min). After 120 min of transfer to warm medium, VacA was observed in vesicles scattered throughout the cytosol (Figure 2C, 120 min). Noteworthy, VacA was never observed clustered in a perinuclear compartment in HeLa or AGS cells after 30 or 120 min of endocytosis.

Figure 2 (cont). zoom 1, arrows: colocalization, between VacA and actin (yellow). After 10 min, VacA started to label tubulovesicular endocytic structures (detected only under permeabilized conditions by contrast to nonpermeabilized cells presented in the bottom row). These compartments are at the top of the cell (zoom 2) or at the cell basal periphery, rear of F-actin structures (zoom 3 and Supplementary Video 3). After 30 min, and moreover after 120 min, VacA was found in vesicular structures scattered throughout the cytosol. (B) Rotation (40° between each frame) in the *Y* plane of a typical tubulovesicular endocytic structure labeled by VacA (extracted from zoom 3 panel A), reconstructed in 3D (see also Supplementary Video 4). (C) AGS cells were process as for HeLa cells. VacA was localized on membrane protrusions (time 0 min). VacA was then endocytosed in a seemingly polarized manner (times 5 and 10 min) and reached larger endocytic compartments at 30 min. After 120 min, the toxin labeled only smaller vesicular compartments scattered throughout the cytosol. Scale bars, 10 μm.

VacA Is Associated with Lipid Rafts in Endocytic Compartments

VacA is documented to bind to lipid rafts (Patel *et al.,* 2002; Schraw *et al.,* 2002; Gauthier *et al.,* 2004). Furthermore, the role of lipid rafts in the VacA cell internalization process was reinforced by the demonstration that depletion of plasma membrane cholesterol by methyl-β-cyclodextrin inhibits cell binding and endocytosis of VacA (Schraw *et al.,* 2002; Patel *et al.,* 2002). On HeLa cells treatment with methyl-β-cyclodextrin, no VacA could be observed in cells after 10 min of endocytosis, although the endocytosis of transferrin was mostly conserved (Supplementary Figure 1D). In AGS cells the different cell endocytic structures reached successively by one wave of the cytotoxin were clearly defined (Figure 2C). We decided to next test the association status between VacA and lipid rafts for 0, 10, 30, and 120 min of endocytosis. As shown in Figure 3A, VacA continued to be found in the low-density fractions after treatment with Triton X-100 and gradient centrifugation, together with the lipid raft marker flottilin 1 but not with transferrin receptor, a nonrafted protein. This suggested that VacA was associated with lipid rafts all along its intracellular trafficking. To further ascertain this point, we took advantage of the recent technique used to demonstrate that the SV40 virus was continuously associated with lipid rafts in endocytic compartments during its intracellular trafficking (Damm *et al.,* 2005). For this purpose, AGS cells were incubated with VacA for 1 h at 4°C, washed and the cytotoxin was endocytosed for 0, 10, 30 and 120 min. For each time, cells were treated or not with Triton X-100 at 4°C, to extract or not nonrafted proteins (as described in *Materials and Methods*). After fixation, cells were processed for the immunofluorescence detection of both VacA and the transferrin receptor. The VacA immunofluorescent signal was present in both the control and Triton X-100-treated preparations (Figure 3B). At difference, the transferrin receptor was only detected in the control preparations (not treated with Triton X-100; Figure 3B), indicating that nonrafted proteins were largely extracted. This suggested that each endocytic compartments reached by VacA contained lipid rafts and that the cytotoxin remained associated with these membrane domains during its endocytosis and intracellular trafficking. The association of VacA in the control and Triton X-100-extracted cell preparations was quantified by immunoblotting. Similar amounts of VacA were associated with cells at the different timings of endocytosis in Triton X-100-extracted or control preparations (Figure 3C). A slight decrease of the VacA amounts was noticed as a function of time (Figure 3C) probably due to degradation of the cytotoxin. At difference, the amounts of transferrin receptor were largely decreased in Triton X-100-extracted preparations compared with flottilin 1 (Figure 3C).

VacA Exploits a Constitutive Actin-dependent Cell Endocytic Pathway Different from Macropinocytosis, Independent of Clathrin, Dynamin, Tyrosine Phosphorylation, RhoA, and Arf6 GTPases Activities

We next studied the effects of factors known to modulate characterized endocytic pathways. Disruption of the F-actin cytoskeleton by cytochalasin D (CD) blocked VacA endocytosis, but not that of transferrin, in both HeLa and AGS cells (Figure 4 A). Expression of the ED95/295 Eps 15 dominant-negative protein in HeLa or AGS cells (Benmerah *et al.,* 1999) blocked the clathrin pathway (as shown by inhibition of the

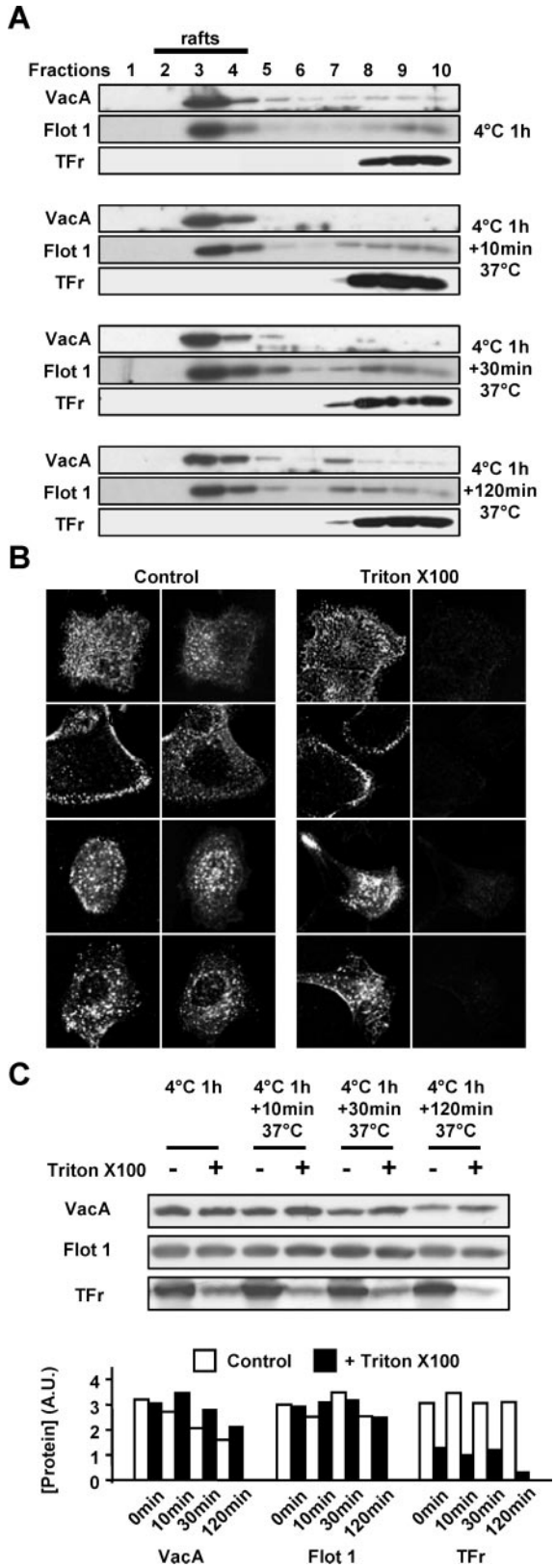

Figure 3. Association of VacA with lipid rafts during endocytosis and intracellular trafficking. (A) AGS cells were incubated with VacA for 1 h at 4°C, washed and warmed for 0, 10, 30, or 120 min at 37°C. For each time point, cells were processed for lipid rafts analysis by flotation gradient after Triton X-100 extraction as described in *Materials and Methods.* Identification of the proteins in each fractions of the gradient was performed by immunoblots using the IgG 958 for VacA, the MAb anti-flotillin 1 for flotillin 1 (Flot 1; a marker of lipid rafts), and the MAb anti-TFr (as a protein marker excluded from lipid rafts). (B) VacA internalized in endocytic compartments is resistant to Triton X-100 extraction at 4°C by contrast to TFr. AGS cells were incubated with VacA at 4°C for 1 h, washed, and incubated for 0, 10, 30 or 120 min at 37°C. Cells were submitted or not to Triton X-100 extraction at 4°C (as described in *Materials and Methods*). Cells were fixed, processed for the detection of VacA and TFr by immunofluorescence, and observed by confocal microscopy. All pictures represent total cell reconstructions from confocal sections. Scale bar, 10 μm. (C) VacA, Flot 1, and TFr protein levels associated with control or Triton X-100-extracted AGS cells. The cells were treated as in B except that after Triton X-100 extraction, they were lysed and analyzed by immunoblots as in A. The histogram represents the quantification of the presented immunoblots (arbitrary units: A.U.).

transferrin endocytosis) without interfering with VacA endocytosis (Figure 4B). Expression of the dominant-negative form of dynamin 2 (Dyn2K44A) in HeLa or AGS cells, which efficiently inhibited the endocytosis of transferrin (Damke *et al.*, 1995; Oh *et al.*, 1998), was without effect on VacA internalization (Figure 4C).

Expression of the dominant-negative form of Arf6 (Arf6 N122I; Honda *et al.*, 1999) did not block VacA endocytosis in HeLa or AGS cells (Figure 5A). Arf6N122I was active because, at difference with the wild-type form of the GTPase that was strictly associated with the cytoplasmic face of the cell plasma membrane (Figure 5A), the mutant was localized in endocytic compartments (Figure 5A) as reported (Honda *et al.*, 1999). Treatment of HeLa (Figure 5B) or AGS cells (unpublished data) by the C3 transferase, to inhibit RhoA activity, did not block VacA internalization. As a control for C3 transferase activity we observed that treated-cells had lost their stress fibers (unpublished data), clearly indicating that RhoA was inhibited (Boquet and Lemichez, 2003).

Many different processes of ligands internalization, through lipid rafts or caveolae, induce and require one or several cellular tyrosine phosphorylation (s) (Parton and Richards, 2003). We tested whether, upon cell binding of VacA, we could detect one or several proteins specifically phosphorylated on tyrosine residues. As shown in Figure 5C, we observed that upon HeLa cell treatment with VacA, no new tyrosine phosphorylation of cellular protein(s) could be observed (in contrast with epidermal growth factor (EGF) treatment). In addition, AGS or HeLa cells treated with the tyrosine kinase inhibitor genistein exhibited a normal pattern of VacA endocytosis (Figure 5B). The effect of genistein was controlled by its ability to block the tyrosine-phosphorylations located in focal adhesion points (unpublished data). We tested whether VacA might provoke its own internalization by triggering macropinocytosis, a process induced upon stimulation with growth factors or other signals. For this purpose we used the measurement of HRP, a bona fide and sensitive marker of fluid phase uptake (Swanson and Watts, 1995), in HeLa cells, in the presence or absence of VacA. As a positive control for macropinocytosis, cells were treated with the tumor promoter agent (TPA) phorbol ester, a known inducer of macropinocytosis (Swanson and Watts, 1995). Although a great increase in HRP uptake was observed in TPA-treated cells, HeLa cells incubated with VacA showed an HRP uptake virtually identical to that of control VacA-untreated cells (Figure 5 D). To further ascertain this point, we tested whether amiloride, a blocker of macropinocytosis (Swanson and Watts, 1995), could inhibit VacA endocytosis. This drug did not inhibit the

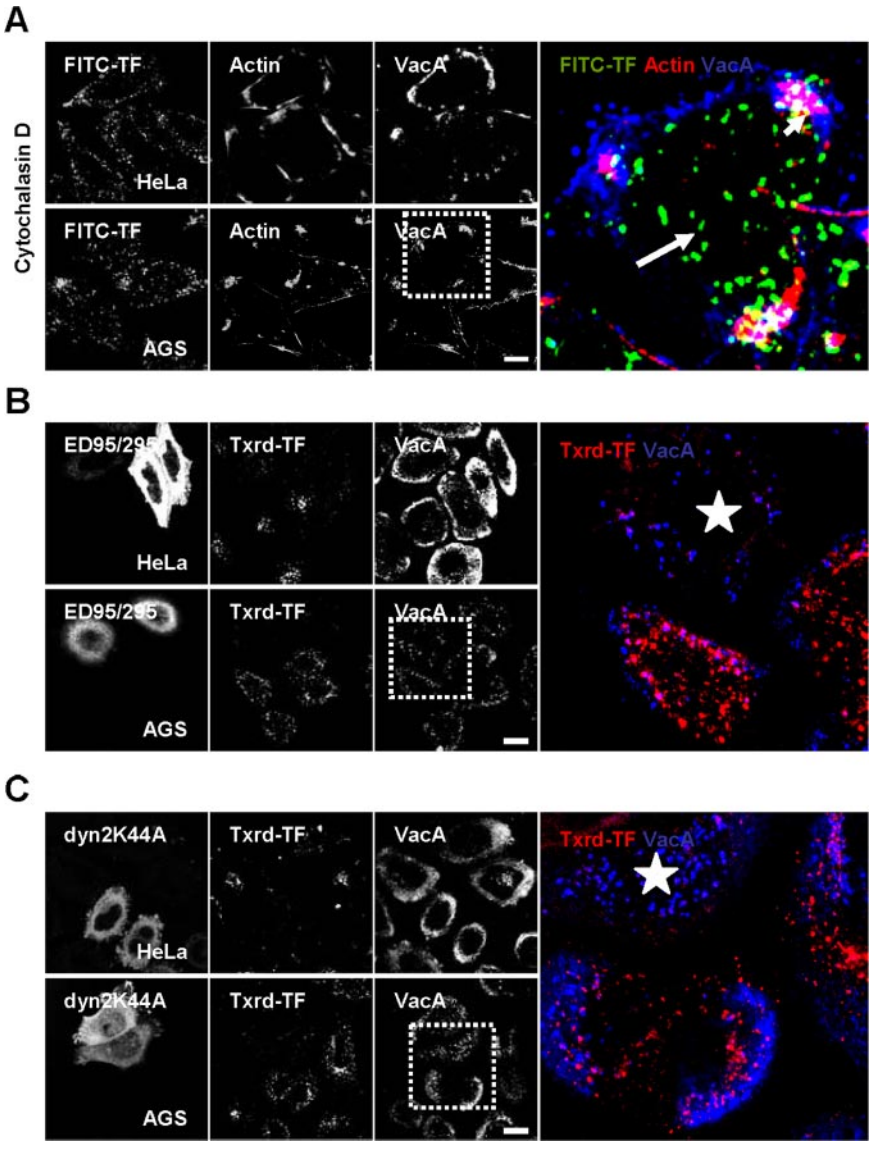

Figure 4. VacA endocytosis is an actin-dependent but clathrin- and dynamin 2-independent mechanism. (A) HeLa or AGS cells were treated with cytochalasin D for 60 min and then rinsed. VacA was added for 1 h at 4°C with FITC-TF. Cells were rinsed and incubated at 37°C for 30 min in the presence of cytochalasin D and then washed, fixed, permeabilized, processed for the detection of VacA, transferrin and actin (TRITC-phalloidin) by immunofluorescence, and observed by confocal microscopy. Small arrows in the zoom show that VacA (blue fluorescence) remained at the surface of cytochalasin D-depolymerized F-actin cells (red, short arrows) at difference with transferrin (green, long arrows). (B and C) HeLa and AGS cells were transfected with the dominant-negative form of Eps15 (ED95/295) or with the dominant-negative form of dynamin 2 (Dyn 2 K44A). VacA was added for 1 h at 4°C together with FITC-transferrin. Cells were rinsed and incubated at 37°C for 30 min, washed, fixed, permeabilized, processed for the detection of VacA and transferrin by immunofluorescence, and then observed by confocal microscopy. In the zooms, stars: transfected cells. All pictures were taken from two confocal sections (HeLa) or a total cell reconstruction from confocal sections (AGS). Scale bars, 10 μm.

entry of VacA into cells (Figure 5B), although it greatly reduced the TPA-induced macropinocytosis of HRP (unpublished data).

These data indicated that VacA did not induce its own internalization but exploited a constitutive cell endocytic pathway different from macropinocytosis, independent of clathrin, dynamin, tyrosine phosphorylation, RhoA, and Arf6 GTPases activities. Therefore, we named this endocytic process "pinocytosis" a term covering all of the cell internalization mechanisms except phagocytosis (Conner and Schmid, 2003).

VacA Is Pinocytosed into Caveolin-, Transferrin-, and EEA1-negative Cell Peripheral Compartments That Contain a Fluid Phase Marker and GPI-Aps

We subsequently studied which endocytic markers were associated with the intracellular VacA-containing compartments observed at the early time point of pinocytosis (10 min). In particular, we investigated whether these compartments were associated with transferrin and the Rab5-effector EEA1 protein, the two classical markers of sorting endosomes (Zerial and McBride, 2001). We also investigated their association with the fluid phase probe dextran and GPI-APs or caveolin 1, which are known markers of endocytic compartments associated with lipid rafts (Pelkmans and Helenius, 2002; Mayor and Riezman, 2004). The cell peripheral intracellular compartments, reached by VacA after 10 min of pinocytosis, did not colocalize with transferrin, EEA1 (Figure 6, A and D) and caveolin 1 detected by a mAb (Figure 6, B and D). However, because the Mab anti-caveolin 1 reacted in immunoblot with several minor bands in addition to the main 22-kDa band, we expressed a GFP-caveolin 1 into cells, to verify that VacA was not associated with caveolin 1 (Supplementary Figure 2A, Supplementary Videos 7 and 8). The cholera B toxin subunit (CTxB), is also a marker of caveosomes (Nichols, 2002). When CTxB and VacA were endocytosed together in HeLa cells for 10 min, no colocalization of the two markers could be observed, whereas CTxB was largely found into caveolin 1-positive compartments (Supplementary Figure 2B). Conversely, a clear colocalization between VacA and the fluid phase marker Txrd-dextran was observed in these compartments (Figure 6, C and D).

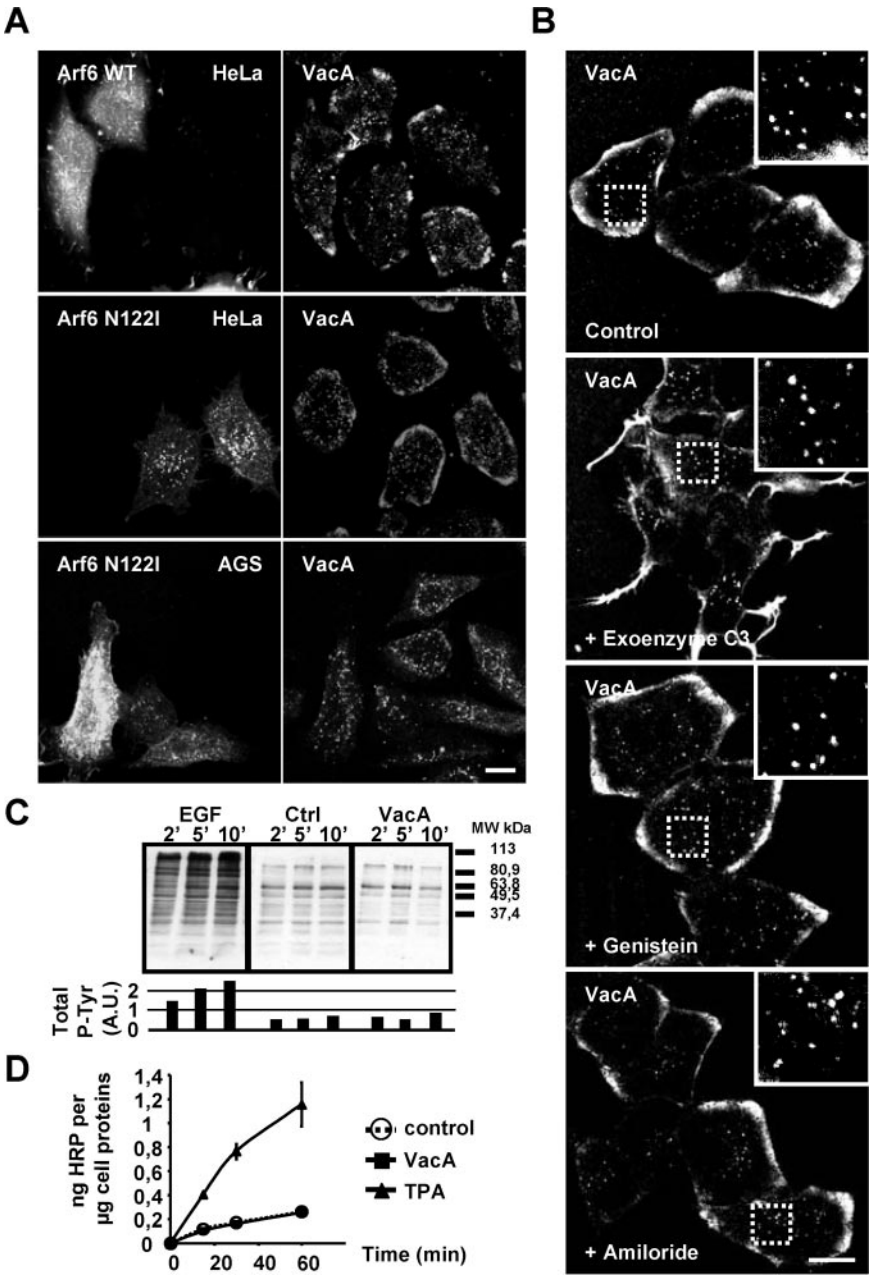

Figure 5. VacA endocytosis does not require Arf6, tyrosine kinase, or RhoA activities, and is different from macropinocytosis. (A) Cells were transfected with the wild-type GFP-Arf6 (Arf6 WT, HeLa cells) or with the dominant negative form of GFP-Arf6 (Arf6 N122I, HeLa and AGS cells). VacA was added for 1 h at 4°C. Cells were rinsed and incubated at 37°C for 30 min, washed, fixed, permeabilized, processed for the detection of VacA and GFP-Arf6 proteins by immunofluorescence, and then observed by confocal microscopy. All pictures represent total cell reconstructions from confocal sections. Scale bar, 10 μm. (B) Treatment of Hela cells with genistein, C3 transferase, or amiloride did not block the endocytosis of VacA. VacA was added to the cells for 1 h at 4°C in each condition (see *Materials and Methods*). Cells were rinsed and incubated at 37°C for 30 min, washed, fixed, permeabilized, and processed for the detection of VacA, actin, or tyrosine-phosphorylation by immunofluorescence. All pictures represent single confocal sections. Vesicles containing VacA are shown in the zooms for the different conditions. Scale bar, 10 μm. (C) Total P-Tyr analysis in HeLa cells. At time 0, serum-starved cells (18 h) were stimulated with EGF (0,66 μg/ml; EGF), untreated (Ctrl), or intoxicated with VacA (VacA); after 2, 5, or 10 min of treatment at 37°C cells were lysed and analyzed by immunoblotting with a Mab anti-phosphotyrosine. The histogram represents the quantification of the total P-Tyr (arbitrary units: A.U.). (D) Horseradish peroxidase (HRP) uptake of control HeLa cells, of cells treated with 30 nM TPA or of cells treated with VacA. Incubation of cells with HRP and assays for HRP cell internalization and detection were performed as described (Steinman and Cohn, 1972).

We next tested whether the cell peripheral early endocytic compartments containing VacA after 10 min of endocytosis contained GPI-APs. On expression of a GPI-GFP (derived from the DAF, see *Materials and Methods*), colocalization between VacA and the GPI-GFP was clearly observed within the cell peripheral early endocytic compartments reached by the cytotoxin (Figure 7A). To demonstrate further the association of endogenous GPI-APs and VacA in these compartments, we used the fluorescent pan-GPI-APs marker ASSP-546, derived from the pore-forming toxin aerolysin (Fivaz *et al.*, 2002). When VacA and ASSP-546 were incubated together with HeLa or AGS cells for 1 h at 4°C and then internalized for 10 min at 37°C, the cytotoxin was colocalized with ASSP-546 in the cell peripheral endocytic compartments (Figure 7B).

Taken together these observations indicated that at an early time point of its endocytosis (10 min) VacA was internalized into cell peripheral compartments devoid of transferrin, caveolin 1, and the EEA1 Rab5 effector but that contained GPI-APs, together with a fluid-phase marker. Such compartments have been described recently as the first station in which non-cross-linked GPI-APs, pinocytosed by a clathrin- and dynamin-independent mechanism, are accumulated at an early time point of their endocytosis (Sabharanjak *et al.*, 2002). These compartments have been named GPI-APs-enriched early endosomal compartments (GEECs; Sabharanjak *et al.*, 2002). VacA appeared thus to be accumulated in GEECs at an early time point (10 min) of endocytosis.

Pinocytosis of VacA Is Controlled by the Cdc42 GTPase

Because VacA pinocytosis is dependent of an intact actin cytoskeleton, we tested whether VacA delivery, after 10 min

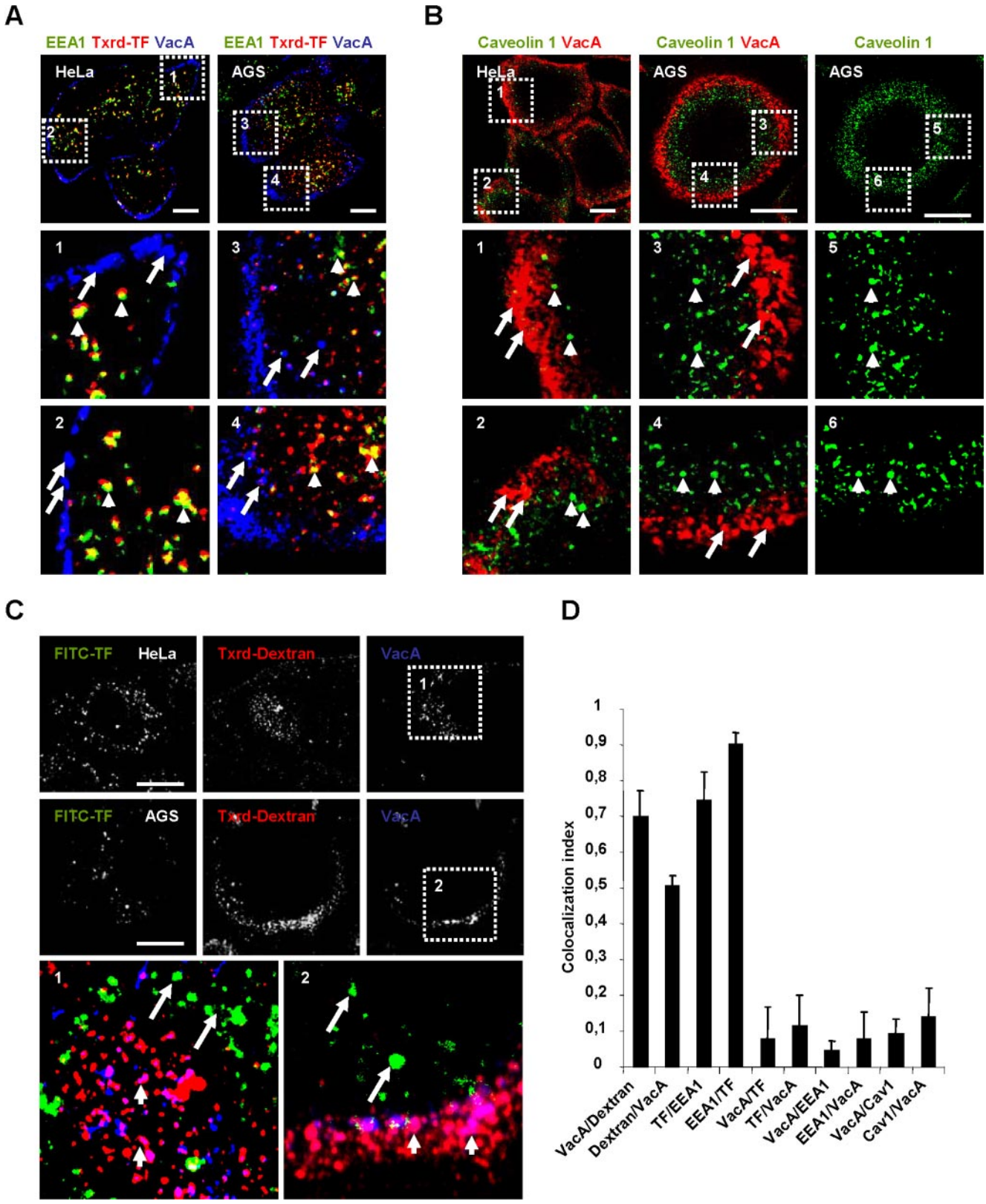

Figure 6. At an early time point of endocytosis VacA reaches an intracellular compartment containing a fluid phase marker, different from early endosomes or caveosomes. (A) AGS or HeLa cells were incubated with VacA and Txrd-T at 4°C for 1 h, washed, and incubated for 10 min at 37°C. Cells were then fixed, permeabilized, and processed for the detection of VacA (blue), the early endosomal marker EEA1 (green). In zooms 1–4, short arrows: EEA1 and transferrin colocalization and long arrows: VacA-positive vesicles. (B) Cells were processed as in A excepted that Caveolin 1 (green) was detected instead of EEA1 and no transferrin was added to the cells. All pictures were taken from single confocal sections and presented for AGS cells with or without the VacA fluorescence (red). In zooms 1–6 short arrows: caveolin 1-coated

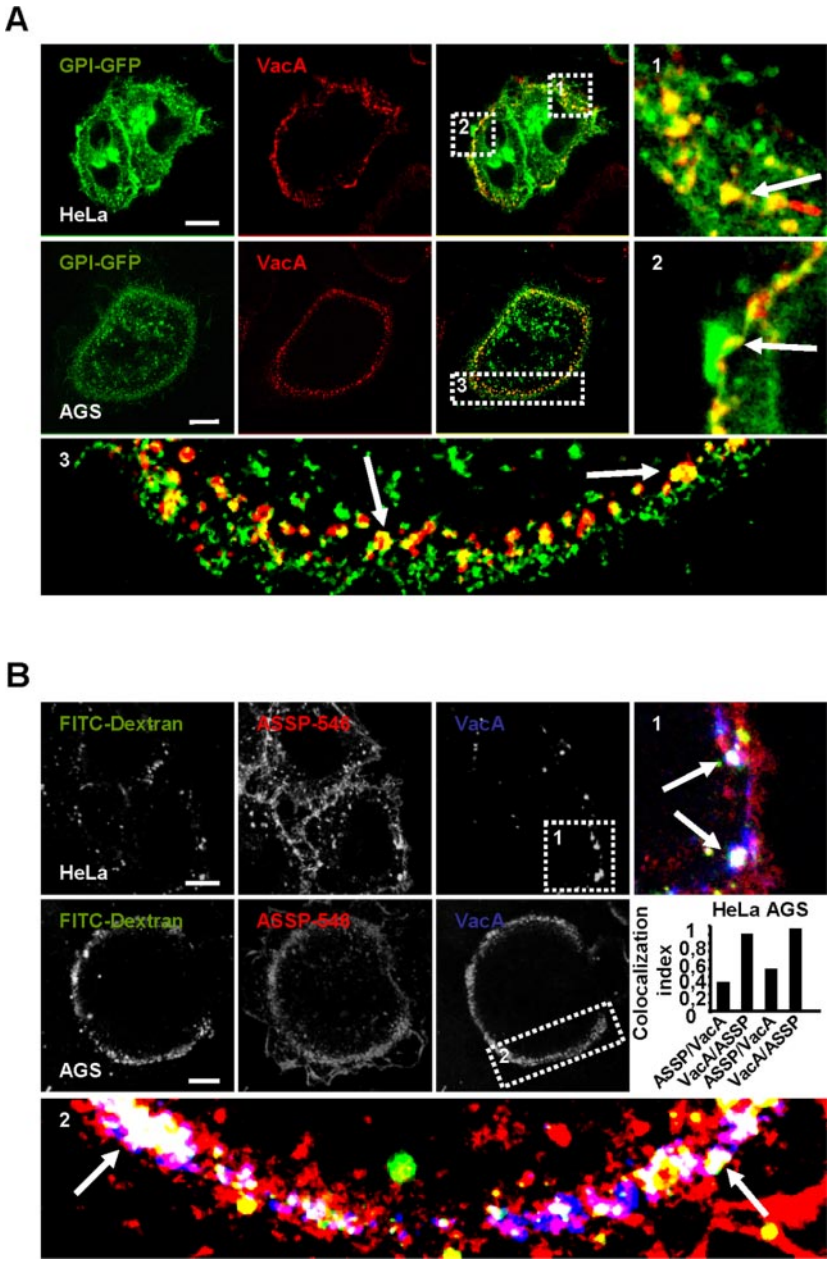

Figure 7. VacA early endocytic compartments contain GPI-APs. (A) HeLa cells or AGS were transfected with GPI-GFP. Cells were incubated at 4°C and VacA was added for 1 h at 4°C. Cells were washed, incubated with VacA in warm medium for 10 min, and then processed for the detection of VacA (red) and GPI-GFP (green) by confocal microscopy. In zooms, arrows indicate the colocalization between VacA and GPI-GFP (yellow). (B) HeLa or AGS cells were incubated at 4°C for 1 h with the pan-GPI-APs marker ASSP-546 and VacA. Cells were washed and incubated in warm medium with FITC-dextran (4 mg/ml) for 10 min and processed for the detection of VacA (blue), ASSP-546 (red), and dextran (green). Arrows in the zooms show the colocalizations (white) between the markers. All pictures in A and B were taken from single confocal sections. Scale bars, 10 μm. The histogram represents the quantification of colocalizations between VacA and ASSP-546 by colocalization index. Results represent the account average for at least 12 cells for each column.

of endocytosis, was controlled by Cdc42 or Rac1 GTPases. Either in HeLa or AGS cells, expression of the dominant-negative form of Cdc42 (Cdc42 T17N) inhibited the VacA and ASSP-546 immunofluorescent signals into the GEECs (Figure 8, A and B). We could, however, detect ASSP-546 or transferrin into vesicles different from those of the GEECs. In contrast, no VacA fluorescent signal could be observed in vesicles containing either transferrin or ASSP-546, after 10 min of pinocytosis, in cells expressing Cdc42 T17N (Figure 8A, zooms 1 and 2). To control that the inhibition of Cdc42 did not affect the cell binding of the cytotoxin, we tested whether VacA was bound on Cdc42 T17N-transfected cells. No gross modification of the cytotoxin binding was observed at 4°C on Cdc42 T17N-transfected compared with untransfected cells (Figure 9, A and B). In particular VacA was bound on long cell protrusions as shown in Figure 1D. In cells expressing Cdc42 T17N, after 10 min at 37°C, VacA remained associated with the long membrane protrusions and did not reach the GEECs as observed in nontransfected cells (Figure 9A). We next tested whether expression of the

Figure 6 (cont). structures and long arrows: VacA-positive vesicles. (C) HeLa or AGS cells were incubated with VacA and FITC-TF at 4°C for 1 h, washed, and incubated for 10 min at 37°C with Txrd-dextran (4 mg/ml). Cells were fixed, permeabilized, and processed for the detection of VacA (blue), transferrin (green), and dextran (red) fluorescences. Pictures were taken from full cell reconstructions using confocal sections. In zooms, short arrows: VacA- and dextran-positive vesicles and long arrows: transferrin-positive vesicles. Scale bars, 10 μm. (D) Quantification of colocalizations between endocytic markers by colocalization index in Hela cells. Results represent an account of at least four cells and each column of the histogram is the average of at least four independent experiments.

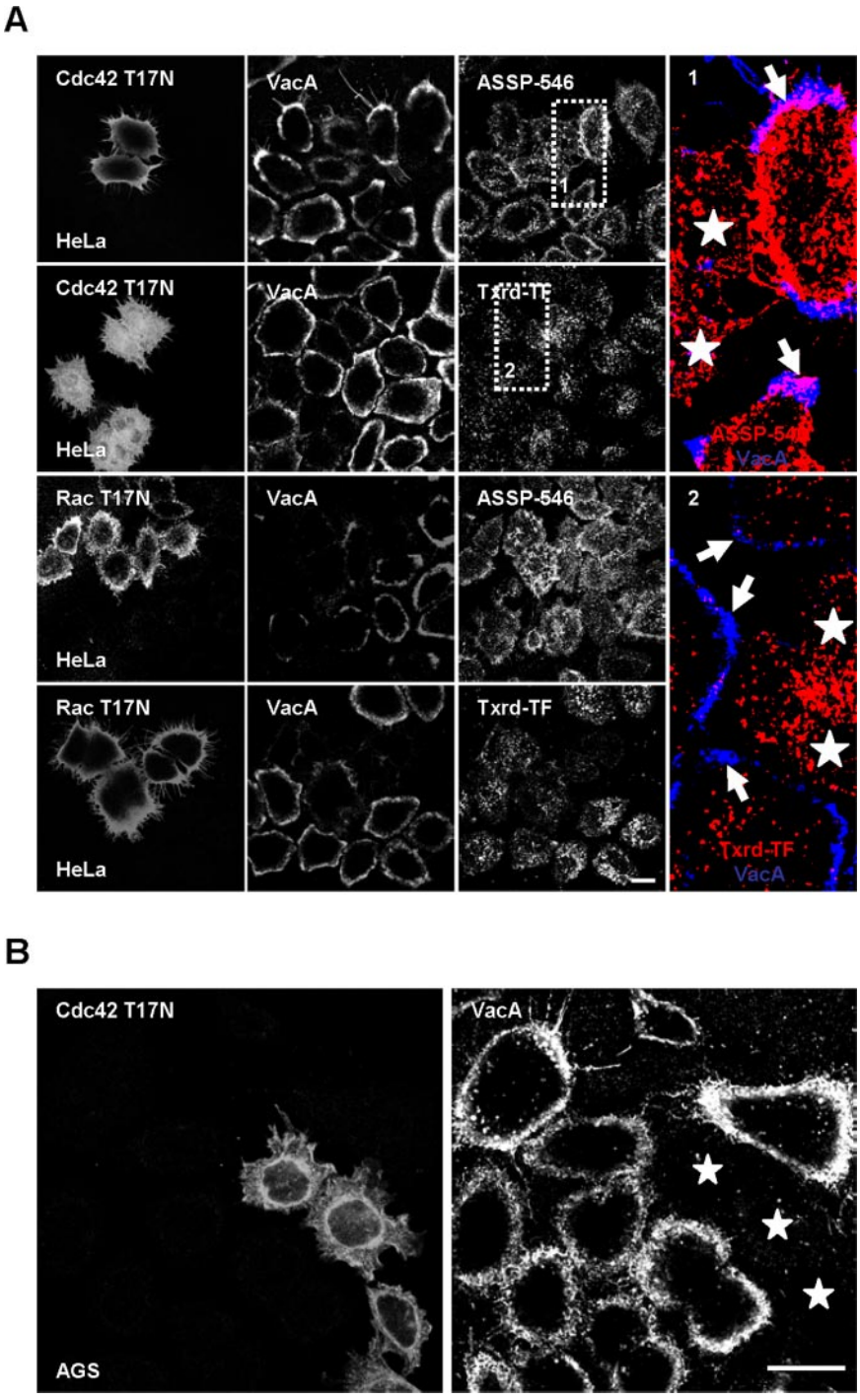

Figure 8. VacA internalization into the GEECs is regulated by the Cdc42 GTPase activity. (A) HeLa cells were transfected with the dominant-negative form of Cdc42 (Cdc42 T17N) or by the dominant-negative form of Rac1 (Rac T17N). VacA was added for 1 h at 4°C together with FITC-TF or ASSP-546. Cells were rinsed and incubated at 37°C for 10 min, washed, fixed, permeabilized, processed for the detection of VacA, transferrin, ASSP-546 and the transfected proteins by immunofluorescence, and then observed by confocal microscopy. In the zooms, stars: transfected cells, VacA: blue, ASSP-546 or transferrin: red. Arrows in zooms 1 show colocalizations between ASSP-546 and VacA in the GEECs and arrows in zoom 2 the GEECs in nontransfected cells. All pictures were taken from one confocal section. Scale bar, 10 μm. (B) Identical as in A, but for the effects of the dominant-negative form of Cdc42 only on VacA endocytosis in AGS cells. Stars: transfected cells. Scale bar, 10 μm.

dominant-negative form of Rac1 (Rac T17N) might inhibit VacA internalization into GEECs. Expression of Rac T17N inhibited the delivery of VacA into the GEECs without modifying the entry of ASSP-546 or transferrin (Figure 8A). A closer examination of RacT17N effects on VacA endocytosis indicated that the dominant-negative form of Rac1 inhibited the fluorescent punctuate pattern of the cytotoxin detected at 4°C on the surface of Hela cells (Figure 9B; same results were obtained with AGS cells' unpublished data). Expression of the dominant-positive form of Rac1 (Rac1 Q61L) reinforced the membrane structures, on which VacA was associated (Figure 9B). Remarkably, there was no increase in VacA cell fluorescence upon expression of the Rac1 Q61L in cells (Figure 9B).

Altogether, these data showed that VacA was bound to the cell surface on F-actin structures, which are localized underneath the plasma membrane and controlled by Rac1. From these structures VacA was pinocytosed into the GEECs by a Cdc42-dependent mechanism and no major rerouting of VacA to the clathrin pathway of endocytosis occurred when the Cdc42 GTPase activity was inhibited. Dependence on the Cdc42 GTPase, for the internalization of VacA into the peripheral cell compartments, reinforced thus the notion that the cytotoxin was taken up into GEECs (Sabharanjak *et al.*, 2002).

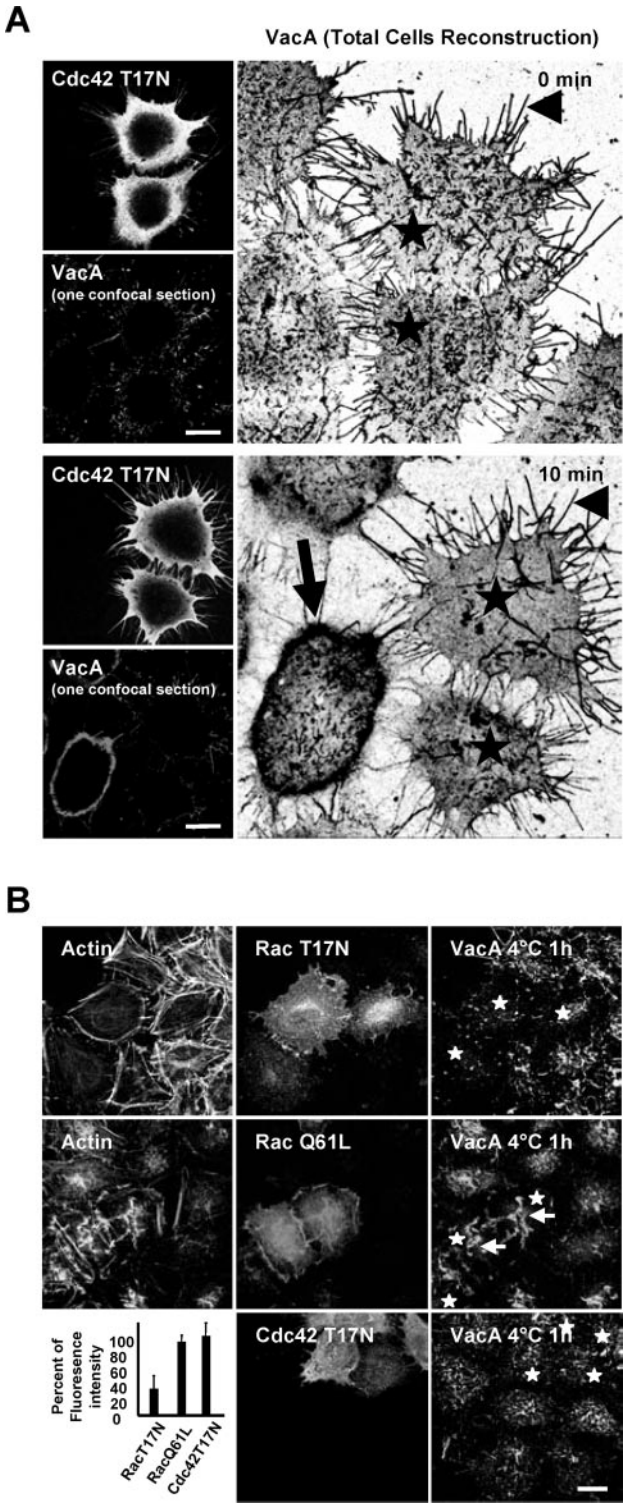

Figure 9. The binding of VacA to the cell surface is regulated by Rac1 but not by Cdc42. (A) Association of VacA with Cdc42 T17N transfected cells. HeLa cells were incubated with VacA at 4°C for 1 h, washed, and incubated for 0 or 10 min at 37°C. Cells were fixed, permeabilized, processed for the detection of VacA and Cdc42 T17N immunofluorescences, and observed by confocal microscopy. At 0 min, VacA is associated with membrane extensions (arrowhead) in both control and transfected cells (stars). After 10 min at 37°C, VacA remained mostly associated with the membrane extensions (arrowhead) of Cdc42 T17N-transfected cells (stars) but was clearly internalized in the GEECs in nontransfected cells (arrow). The large pictures show a negative black and white total cell reconstruction. The small pictures show one medial confocal section of the corresponding fields of the large pictures for Cdc42 T17N and VacA fluorescences. (B) HeLa cells were transfected with either the dominant-negative form of Rac1 (Rac T17N), Cdc42 (Cdc42 T17N), or by the dominant-positive form of Rac1 (Rac Q61L). Cells were incubated with VacA for 1 h at 4°C. Cells were washed, fixed, and processed for immunofluorescence of actin, VacA, Rac1, or Cdc42. The pictures were taken from full cell reconstructions using confocal sections. The histogram represents the quantification of VacA fluorescence associated with the whole cell surface. For this purpose cells were reconstructed totally using confocal sections. Each cell area was determined using the fluorescence pattern of F-actin. This area was used to delimit the VacA fluorescence at the surface of each cell. The total fluorescence level of VacA was quantified. The results are expressed as a difference between VacA fluorescence level on transfected cells and that of surrounded untransfected cells (results are express in %, untransfected cells being taken as the 100% for each transfected construction). Quantifications were performed using the Metamorph software. Results represent the account average of three independent experiences. Scale bars, 10 μm.

VacA Is Sorted from the GEECs to the Degradative Pathway

We next analyzed the intracellular compartment to which VacA was transferred after reaching the GEECs. In HeLa cells, upon 30 min of endocytosis at 37°C, some vesicular structures were observed scattered throughout the cytosol (away from the GEECs), colocalized with the Rab5 effector EEA1 (Figure 10A) and not with endogenous caveolin 1 positive vesicles (Supplementary Figure 1C). However, one part of the VacA immunofluorescent signal was however still confined to the GEECs (Figure 10A). The scenario was different in AGS cells: after 30 min of endocytosis most of the VacA immunofluorescent signal was transferred from GEECs to large EEA1-positive vesicles (Figure 10A).

From 30 to 120 min the cytotoxin molecules were progressively transferred from sorting endosomes to the LAMP1 compartment (Figure 10B). After 120 min, VacA-positive vesicles colocalized almost entirely with the late endosomal/lysosomal marker LAMP1 (Griffith *et al.*, 1988; Figure 10, A and B).

DISCUSSION

In HeLa and AGS cells, VacA was observed to bind to actin-rich membrane extensions at 4°C. We have shown that formation of these VacA-associated F-actin-rich membrane structures was controlled by the Rac1 but not by the Cdc42 GTPase. Indeed, upon expression of the dominant-negative form of Rac1, association of VacA on the cell plasma membrane was abolished but conversely concentrated on membrane folds upon expression of the dominant-positive form of the GTPase. These observations are in agreement with the report that expression of the dominant-negative form of Rac1 (RacT17N) inhibits the VacA-induced cell vacuolation (Hotchin *et al.*, 2000). Interestingly, the transmembrane proteoglycan syndecan-4, a receptor for the fibroblast growth factor 2 (FGF2) also requires the activity of Rac1 to cluster FGF2 at the cell surface before pinocytosis (Tkachenko *et al.*, 2004).

VacA pinocytosis did not require tyrosine phosphorylation of cellular proteins and was independent of RhoA, dynamin 2, and ARF6 GTPases activities. This process differs from most lipid rafts/caveolae-dependent endocytic pathways (Parton and Richards, 2003). We have shown that no increase in the cell fluid phase uptake could be detected

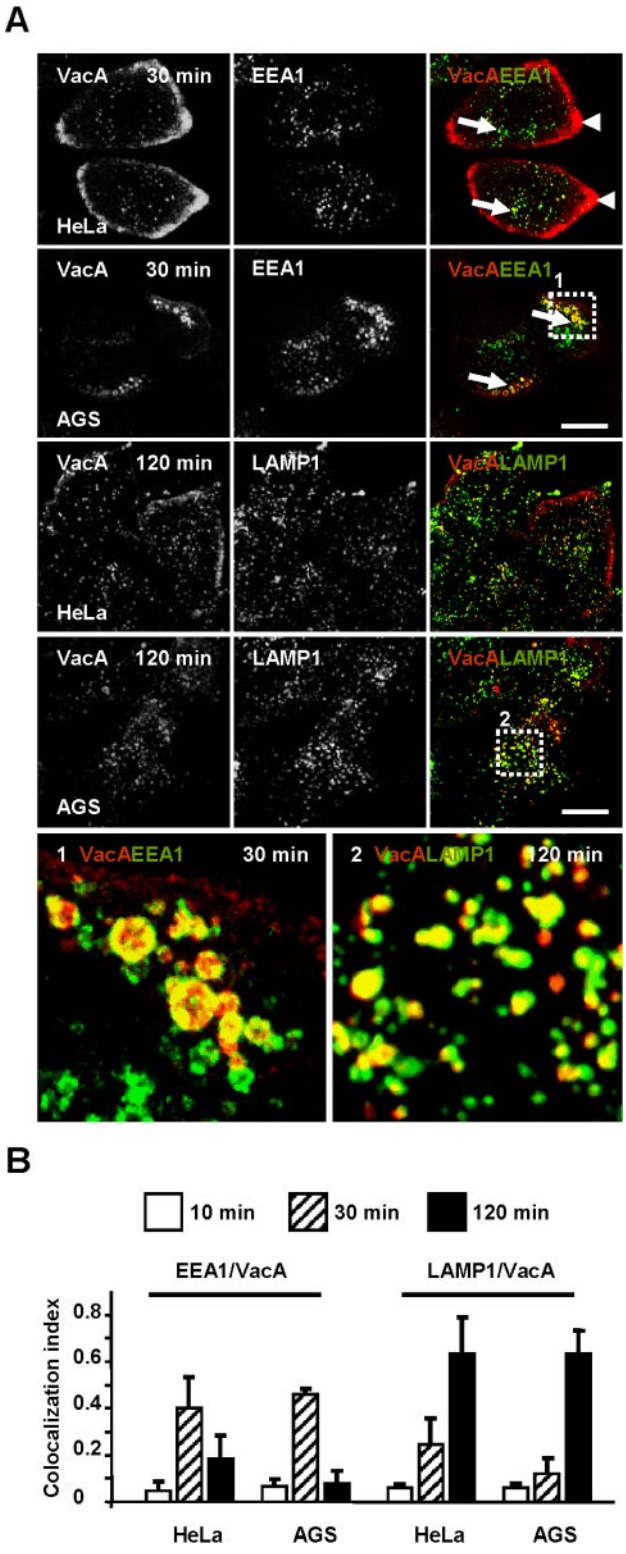

Figure 10. VacA is transferred from the GEECs to EEA1-positive sorting endosomes and subsequently routed to LAMP1-positive vesicles. (A) HeLa cells or AGS cells were incubated with VacA at 4°C for 1 h, washed, and incubated for 30 or 120 min at 37°C. Cells were processed for the detection of VacA (red), EEA1 (green at 30 min), and LAMP1 (green at 120 min), by indirect immunofluorescence. Long arrows: VacA colocalization with sorting early endosome labeled with EEA1 (yellow). Arrowheads: VacA in the GEECs. Zoom 1 shows the detail colocalization of VacA with EEA1-positive endocytic vesicles in AGS cells. Zoom 2 shows the detail colocalization of VacA with LAMP1-positive endocytic vesicles in AGS cells. The images were taken from full-cell reconstructions using confocal sections. Scale bars, 10 μm. (B) Quantification of colocalizations between endocytic markers by colocalization index. Results represent an account of at least six cells and each column of the histogram is the average of at least three independent experiments.

upon VacA intoxication. Furthermore, pinocytosis of VacA was not inhibited by amiloride, a blocker of macropinocytosis (Swanson and Watts, 1995). Consequently VacA pinocytosis is probably not induced by the cytotoxin and thus not a macropinocytic process. Thus, VacA exploits most likely a cell constitutive mechanism of pinocytosis.

Membrane-bound toxin molecules were found inside the cell after 10 min at 37°C, associated with vacuolar compartments predominantly localized just underneath the cytoplasmic face of the membrane. In particular, these compartments were tubulovesicular structures localized at the cell periphery. Those structures bear morphological similarities with GEECs (Sabharanjak *et al.*, 2002). In support that VacA is pinocytosed into GEECs, we observed that the cytotoxin was found after 10 min of pinocytosis in intracellular compartments containing GPI-APs together with a fluid phase tracer (fluorescent dextran). These compartments were, as shown for GEECs (Sabharanjak *et al.*, 2002), devoid of transferrin, and of the Rab5 effector protein EEA1. In contrast to VacA, at the same time point of 10 min, transferrin colocalized with the EEA1 marker, indicating that this molecule had already reached EEA1-early endosomes, likely by the clathrin-dependent pathway.

The early endocytic cell peripheral compartments reach by VacA were not caveosomes (Pelkmans and Helenius, 2002), which have been implicated in the transport of SV40 virus, GPI-APs, CTxB, and Shiga toxin B subunits from the plasma membrane to the Golgi apparatus (Nichols, 2002). Indeed, VacA was never observed colocalized with endogenous caveolin-1-positive vesicles (even after 30 min of pinocytosis) or with CTxB. In mouse embryonic fibroblasts, it was recently reported that a portion of membrane-bound CTxB reaches tubulovesicular structures with resembling features of GEECs before being routed to the *trans*-Golgi network (Kirkham *et al.*, 2005). The fact that we did not observe a colocalization between VacA and CTxB after 10 min of endocytosis may be due to the difference of cell types (human epithelial cells vs. mouse embryonic fibroblasts).

Pinocytosis of GPI-APs into GEECs is controlled by the Cdc42 GTPase activity (Sabharanjak *et al.*, 2002; Mayor and Riezman, 2004) and dependence on the Cdc42 is a main feature of the GEECs pathway (Mayor and Riezman, 2004). In agreement that VacA is pinocytosed into GEECs, we found that expression of the dominant-negative form of Cdc42 (Cdc42 T17N) blocked the internalization of the cytotoxin. Pinocytosis of VacA might thus follow the internalization process described for non-cross-linked GPI-APs (Sabharanjak *et al.*, 2002). In favor of this hypothesis, intracellular expression of a GPI-AP results in an increased of VacA endocytosis (Kuo and Wang, 2003). At difference, hamster ovary cells (Chinese Hamster ovary [CHO]) deficient of GPI-APs were shown to exhibit a sensitivity similar to high concentrations (25 μg/ml) of VacA compared with their wild-type counterparts (Schraw *et al.*, 2002). However, it should be noted that CHO cells have been classified as highly resistant cells to VacA (Leunk *et al.*, 1988), suggesting that they may lack a specific receptor for the cytotoxin or may use a less efficient endocytic process than HeLa or AGS

cells. At difference with GPI-APs, which upon Cdc42 T17N expression are shifted to the clathrin-dependent pathway (Sabharanjak *et al.,* 2002), VacA was not rerouted to the transferrin-containing endosomes, because we did not observe any accumulation of the toxin in Cdc42 T17N-transfected cells. One possible explanation might be that the VacA receptor(s) is totally excluded from coated pit.

It is interesting to discuss our results with the different views on the clathrin-independent endocytic routes described for GPI-APs to date (Nichols, 2002; Sabharanjak *et al.,* 2002). According to the findings of Sabharanjak *et al.* (2002) non-cross-linked GPI-APs are rapidly internalized into peripheral tubulovesicular compartments (GEECs) that accumulate fluid phase markers but devoid of transferrin. Importantly, pinocytosis of GPI-APs in GEECs does not depend on dynamin and caveolin-1 but is controlled by the Cdc42 GTPase (Sabharanjak *et al.,* 2002). From the GEECs, GPI-APs are then routed back to the cell surface via their transfer to recycling endosomes. At difference, Nichols (2002) proposes that GPI-APs, upon their internalization from the plasma membrane by caveolae invaginations, reach caveosomes. From caveosomes GPI-APs are transferred to the Golgi apparatus by caveolin-1-negative vesicles and subsequently are sent back to the cell surface. Although VacA is not a GPI-AP and given that GPI-APs are not receptors for the cytotoxin, GPI-APs seem instrumental in the endocytosis of VacA (Ricci *et al.,* 2000; Kuo and Wang, 2003; Gauthier *et al.,* 2004). Pinocytosis of VacA into GEECs fits thus quite well with the endocytosis of non-cross-linked GPI-APs described by the Mayor's group (Sabharanjak *et al.,* 2002; Mayor and Riezman, 2004).

Late endosomes as a final destination for VacA endocytosis is well described (Papini *et al.,* 2001). However, the early steps of VacA pinocytosis have not yet been documented. As we described above, after 10 min of pinocytosis, VacA was into GEECs. The GEECs are described as early endosomal compartments connected to recycling endosomes for the internalization of non-cross-linked GPI-APs (Sabharanjak *et al.,* 2002; Mayor and Riezman, 2004). At difference, VacA was exclusively routed from GEECs to EEA1-positive early endosomes (sorting endosomes; Zerial and McBride, 2001) and never observed into a pericentriolar compartment (recycling compartment). From sorting endosomes, the cytotoxin was transferred to the degradative pathway. As a working hypothesis, we suggest that within the GEECs, the tight association of VacA with lipid rafts might be the signal for the selective transfer of the cytotoxin to the degradative pathway. With regard to this hypothesis, it has been shown that in BHK cells the high affinity of GPI-APs for lipid rafts (that increases their time of residency into rafts) was a signal for their selective sorting from GEECs to the degradative pathway (Fivaz *et al.,* 2002). Interestingly, GPI-APs, detected by ASSP-546, were found associated with lipid rafts also in late endosomes of BHK cells (Fivaz *et al.,* 2002). In this respect, we found that VacA was continuously associated with detergent resistant membrane domains during its intracellular trafficking. This may further support the notion that the sorting signal into GEECs for the transfer of VacA to the degradative pathway could be a tight association of the cytotoxin with lipid rafts.

ACKNOWLEDGMENTS

We thank Y. Le Marchand-Brustel, M. Cormont (INSERM U568) and the Bettencourt-Schueller's foundation for videomicroscopy facilities and J. Vukmirica (INSERM U568) for critical reading of the manuscript. P.M. was supported by the Ligue Nationale Contre le Cancer and by the Association pour la Recherche sur le Cancer (ARC). V.K. was supported by the Fondation pour la Recherche Medicale. This work, in partial fulfillment of N.C.G.'s PhD thesis, was funded by the Institut National de la Santé et de la Recherche Médicale (INSERM, Paris, France) and from a grant (number 3484) from the ARC to P.B.

REFERENCES

Adair, W. L., and Kornfeld, S. (1974). Isolation of the receptors for wheat germ agglutinin and the *Ricinus communis* lectins from human erythrocytes using affinity chromatography. J. Biol. Chem. *249*, 4696–4704.

Benmerah, A., Bayrou, M., Cerf-Bensussan, N., and Dautry-Varsat, A. (1999). Inhibition of clathrin-coated pit assembly by an Eps15 mutant. J. Cell Sci. *112*, 1303–1311.

Blanke, S. R. (2005). Micro-managing the executioner: pathogen targeting of mitochondria. Trends Microbiol. *13*, 64–71.

Blaser, M. J., and Atherton, J. C. (2004). *Helicobacter pylori* persistence: biology and disease. J. Clin. Invest. *113*, 321–333.

Boquet, P., and Lemichez, E. (2003). Bacterial virulence factors targeting Rho GTPases: parasitism or symbiosis? Trends Cell Biol. *13*, 238–246.

Boquet, P., Ricci, V., Galmiche, A., and Gauthier, N. C. (2003). Gastric cell apoptosis and *H. pylori*: has the main function of VacA finally been identified? Trends Microbiol. *11*, 410–413.

Conner, S. D., and Schmid, S. L. (2003). Regulated portals of entry into the cell. Nature *422*, 37–44.

Cover, T. L. (1996). The vacuolating cytotoxin of *Helicobacter pylori.* Mol. Microbiol. *20*, 241–246.

Cover, T. L., and Blanke, S. R. (2005). *Helicobacter pylori* VacA, a paradigm for toxin multifunctionality. Nat. Rev. Microbiol. *3*, 320–332.

Cover, T. L., and Blaser, M. J. (1992). Purification and characterization of the vacuolating toxin from *Helicobacter pylori.* J. Biol. Chem. *267*, 10570–10575.

Czajkowsky, D. M., Iwamoto, H., Cover, T. L., and Shao, Z. (1999). The vacuolating toxin from *Helicobacter pylori* forms hexameric pores in lipid bilayers at low pH. Proc. Natl. Acad. Sci. USA *96*, 2001–2006.

Damke, H., Baba, T., van der Bliek, A. M., and Schmid, S. L. (1995). Clathrin-independent pinocytosis is induced in cells overexpressing a temperature-sensitive mutant of dynamin. J. Cell Biol. *131*, 69–80.

Damm, E. M., Pelkmans, L., Kartenbeck, J., Mezzacasa, A., Kurzchalia, T., and Helenius, A. (2005). Clathrin- and caveolin-1-independent endocytosis: entry of simian virus 40 into cells devoid of caveolae. J. Cell Biol. *168*, 477–488.

de Bernard, M., Papini, E., de Filippis, V., Gottardi, E., Telford, J., Manetti, R., Fontana, A., Rappuoli, R., and Montecucco, C. (1995). Low pH activates the vacuolating toxin of *Helicobacter pylori*, which becomes acid and pepsin resistant. J. Biol. Chem. *270*, 23937–23940.

Doye, A., Mettouchi, A., Bossis, G., Clement, R., Buisson-Touati, C., Flatau, G., Gagnoux, L., Piechaczyk, M., Boquet, P., and Lemichez, E. (2002). CNF1 exploits the ubiquitin-proteasome machinery to restrict Rho GTPase activation for bacterial host cell invasion. Cell *111*, 553–564.

Fivaz, M., Vilbois, F., Thurnheer, S., Pasquali, C., Abrami, L., Bickel, P. E., Parton, R. G., and van der Goot, F. G. (2002). Differential sorting and fate of endocytosed GPI-anchored proteins. EMBO J. *21*, 3989–4000.

Galmiche, A. *et al.* (2000). The N-terminal 34 kDa fragment of *Helicobacter pylori* vacuolating cytotoxin targets mitochondria and induces cytochrome c release. EMBO J. *19*, 6361–6370.

Garner, J. A., and Cover, T. L. (1996). Binding and internalization of the *Helicobacter pylori* vacuolating cytotoxin by epithelial cells. Infect. Immun. *64*, 4197–4203.

Gauthier, N. C., Ricci, V., Gounon, P., Doye, A., Tauc, M., Poujeol, P., and Boquet, P. (2004). Glycosylphosphatidylinositol-anchored proteins and actin cytoskeleton modulate chloride transport by channels formed by the *Helicobacter pylori* vacuolating cytotoxin VacA in HeLa cells. J. Biol. Chem. *279*, 9481–9489.

Griffith, G., Hoflack, B., Simons, K., Mellman, I., and Kornfeld, S. (1988). The mannose-6-phosphate receptor and the biogenesis of lysosomes. Cell *52*, 329–341.

Honda, A. *et al.* (1999). Phosphatidylinositol 4-phosphate 5-kinase alpha is a downstream effector of the small G protein ARF6 in membrane ruffle formation. Cell *99*, 521–532.

Hotchin, N. A., Cover, T. L., and Akhtar, N. (2000). Cell vacuolation induced by the VacA cytotoxin of *Helicobacter pylori* is regulated by the Rac1 GTPase. J. Biol. Chem. *275*, 14009–14012.

Kirkham, M., Fujita, A., Chadda, R., Nixon, S. J., Kurzchalia, T. V., Sharma, D. K., Pagano, R. E., Hancock, J. F., Mayor, S., and Parton, R. G. (2005). Ultrastructural identification of uncoated caveolin-independent early endocytic vehicles. J. Cell Biol. *24*, 465–476.

Kuo, C. H., and Wang, W. C. (2003). Binding and internalization of *Helicobacter pylori* VacA via cellular lipid rafts in epithelial cells. Biochem. Biophys. Res. Commun. *303*, 640–644.

Lafont, F., Abrami, L., and van der Goot, F. G. (2004). Bacterial subversion of lipid rafts. Curr. Opin. Microbiol. *7*, 4–10.

Leunk, R. D., Johnson, P. T., David, B. C., Kraft, W. G., and Morgan, D. R. (1988). Cytotoxic activity in broth-culture filtrates of *Campylobacter pylori.* J. Med. Microbiol. *26*, 93–99.

Li, Y., Wandinger-Ness, A., Goldenring, J. R., and Cover, T. L. (2004). Clustering and redistribution of late endocytic compartments in response to *Helicobacter pylori* vacuolating toxin. Mol. Biol. Cell *15*, 1946–1959.

Maxfield, F. R., and McGraw, T. E. (2004). Endocytic recycling. Nat. Rev. Mol. Cell. Biol. *5*, 121–132.

Mayor, S., and Riezman, H. (2004). Sorting GPI-anchored proteins. Nat. Rev. Mol. Cell. Biol. *5*, 110–120.

Nichols, B. J. (2002). A distinct class of endosome mediates clathrin-independent endocytosis to the Golgi complex. Nat. Cell Biol. *4*, 374–378.

Oh, P., McIntosh, D. P., and Schnitzer, J. E. (1998). Dynamin at the neck of caveolae mediates their budding to form transport vesicles by GTP-driven fission from the plasma membrane of endothelium. J. Cell Biol. *141*, 101–114.

Pagliaccia, C., de Bernard, M., Lupetti, P., Ji, X., Burroni, D., Cover, T. L., Papini, E., Rappuoli, R., Telford, J. L., and Reyrat, J. M. (1998). The m2 form of the *Helicobacter pylori* cytotoxin has cell type-specific vacuolating activity. Proc. Natl. Acad. Sci. USA *95*, 10212–10217.

Papini, E., de Bernard, M., Milia, E., Bugnoli, M., Zerial, M., Rappuoli, R., and Montecucco, C. (1994). Cellular vacuoles induced by *Helicobacter pylori* originate from late endosomal compartments. Proc. Natl. Acad. Sci. USA *91*, 9720–9724.

Papini, E., Zoratti, M., and Cover, T. L. (2001). In search of the *Helicobacter pylori* VacA mechanism of action. Toxicon *39*, 1757–1767.

Parton, R. G., and Richards, A. A. (2003). Lipid rafts and caveolae as portals for endocytosis: new insights and common mechanisms. Traffic *4*, 724–738.

Patel, H. K., Willhite, D. C., Patel, R. M., Ye, D., Williams, C. L., Torres, E. M., Marty, K. B., MacDonald, R. A., and Blanke, S. R. (2002). Plasma membrane cholesterol modulates cellular vacuolation induced by the *Helicobacter pylori* vacuolating cytotoxin. Infect. Immun. *70*, 4112–4123.

Pelkmans, L., and Helenius, A. (2002). Endocytosis via caveolae. Traffic *3*, 311–320.

Ricci, V., Galmiche, A., Doye, A., Necchi, V., Solcia, E., and Boquet, P. (2000). High cell sensitivity to *Helicobacter pylori* VacA toxin depends on a GPI-anchored protein and is not blocked by inhibition of the clathrin-mediated pathway of endocytosis. Mol. Biol. Cell *11*, 3897–3909.

Ricci, V., Sommi, P., Fiocca, R., Romano, M., Solcia, E., and Ventura, U. (1997). *Helicobacter pylori* vacuolating toxin accumulates within the endosomal-vacuolar compartment of cultured gastric cells and potentiates the vacuolating activity of ammonia. J. Pathol. *183*, 453–459.

Sabharanjak, S., Sharma, P., Parton, R. G., and Mayor, S. (2002). GPI-anchored proteins are delivered to recycling endosomes via a distinct cdc42-regulated, clathrin-independent pinocytic pathway. Dev. Cell *2*, 411–423.

Salama, N. R., Otto, G., Tompkins, L., and Falkow, S. (2001). Vacuolating cytotoxin of *Helicobacter pylori* plays a role during colonization in a mouse model of infection. Infect. Immun. *69*, 730–736.

Schraw, W., Li, Y., McClain, M. S., van der Goot, F. G., and Cover, T. L. (2002). Association of *Helicobacter pylori* vacuolating toxin (VacA) with lipid rafts. J. Biol. Chem. *277*, 34642–34650.

Steinman, R. M., and Cohn, Z. A. (1972). The interaction of soluble horseradish peroxidase with mouse peritoneal macrophages in vitro. J. Cell Biol. *55*, 186–204.

Swanson, J. A., and Watts, C. (1995). Macropinocytosis. Trends Cell Biol. *5*, 424–428.

Szabo, I., Brutsche, S., Tombola, F., Moschioni, M., Satin, B., Telford, J. L., Rappuoli, R., Montecucco, C., Papini, E., and Zoratti, M. (1999). Formation of anion-selective channels in the cell plasma membrane by the toxin VacA of *Helicobacter pylori* is required for its biological activity. EMBO J. *18*, 5517–5527.

Tkachenko, E., Lutgens, E., Stan, R.V., and Simons, M. (2004). Fibroblast growth factor 2 endocytosis in endothelial cells proceed via syndecan-4-dependent activation of Rac1 and a Cdc42-dependent macropinocytic pathway. J. Cell Sci. *117*, 3189–3199.

Tombola, F., Carlesso, C., Szabo, I., de Bernard, M., Reyrat, J. M., Telford, J. L., Rappuoli, R., Montecucco, C., Papini, E., and Zoratti, M. (1999). *Helicobacter pylori* vacuolating toxin forms anion-selective channels in planar lipid bilayers: possible implications for the mechanism of cellular vacuolation. Biophys. J. *76*, 1401–1419.

Willhite, D. C., and Blanke, S. R. (2004). *Helicobacter pylori* vacuolating cytotoxin enters cells, localizes to the mitochondria, and induces mitochondrial membrane permeability changes correlated to toxin channel activity. Cell. Microbiol. *6*, 143–154.

Zerial, M., and McBride, H. (2001). Rab proteins as membrane organizers. Nat. Rev. Mol. Cell. Biol. *2*, 107–117.